B. ŽUŽEK, F. KAFEXHIU, B. PODGORNIK, F. VODOPIVEC

ISSN 0543-5846
METABK 56(3-4) 323-325 (2017)
UDC – UDK 669.15:620.18:661.665:620.17=111

EFFECT OF CARBIDES SIZE AND DISTRIBUTION ON CREEP RATE

Received – Primljeno: 2016-11-18
Accepted – Prihvaćeno: 2017-03-28
Original Scientific Paper – Izvorni znanstveni rad

One of the most influential microstructure constituents in creep resistant steels are carbide particles. Carbide particles act as obstacles to dislocations movement, therefore the creep rate strongly depends on their size and distribution. At elevated temperatures to which creep resistant steels are exposed, carbide morphology is altered by the coarsening mechanism, consequently deteriorating the creep resistance of these steels. The aim of this work is to study the role of size and distribution of carbide particles on creep rate. Different distributions and size of carbides were obtained by different heat treatment conditions. The effect of different carbide morphology on the creep resistance was evaluated by uniaxial constant load creep tests.

Keywords: alloy steels, microstructure, carbide particles, mechanical properties, creep resistance

INTRODUCTION

Some of vital components in thermal power plants that endure the highest thermal and mechanical service loads are produced from tempered martensitic ferritic steels with 9 – 12 % Cr [1–4]. Chromium is an important alloying element, it promotes ferrite, increases corrosion resistance and is a strong carbide former [5, 6].

These widely used steels operate at temperatures between 773 and 923 K (500 – 650 °C). During service lifetime these steels are exposed to high loads, high temperatures, corrosive environment, thermal shocks, etc., conditions that induce degradation of their microstructure, which in turn limits their lifetime. Therefore a detailed understanding of these processes and the role of microstructure is essential [7-9].

Tempered martensitic microstructure of these steels is obtained by quenching and subsequent one- or two-step tempering. Beside optimal chemical composition, heat treatment parameters have a crucial role in obtaining the appropriate tempered martensitic microstructure with finely dispersed carbide particles [10].

Carbide particles behave as obstacles to dislocations movement, with the creep rate strongly depending on their size and distribution. In previous studies it was proven that these parameters govern the velocity of dislocation movement, which affects the creep resistance of these steels [11, 12].

At elevated temperatures, to which creep resistant steels are exposed, carbides coarsen, [11-13] i.e., some of them grow and others dissolve, consequently deteriorating the steel's creep resistance. The aim of present work was to analyze the role of size and distribution of carbide particles on creep resistance of three grades of 9 – 12 % Cr steels. With different heat treatment parameters, different distribution and size of carbides was obtained. In order to study the effect of these microstructure features, creep test were performed following the heat treatment.

B. Žužek, F. Kafexhiu, B. Podgornik, F. Vodopivec, Institute of Metals and Technology, Ljubljana, Slovenia

EXPERIMENTAL

The steels used in this investigation belong to the group of 9 – 12 % chromium creep-resistant steels. The microstructure and its effect on creep rate of the steels X20CrMoV12-1, X10CrMoVNb9-1, and X12CrMoWVNbN10-1-1were investigated. The microstructure of investigates steels was examined using the JEOL JSM6500F electron microscope. The chemical composition of the investigated steels is given in Table 1.

Table 1 **Chemical composition of the investigated steels / wt. %**

Steel	X20Cr-MoV-12-1	X10Cr-MoV-Nb9-1	X12Cr- MoW-VNb-N10-1-1
C	0,23	0,12	0,12
Si	0,21	0,34	0,07
Mn	0,64	0,48	0,44
Cr	10,33	8,51	10,10
Mo	0,90	0,92	1,03
Ni	0,72	0,09	0,73
V	0,30	0,25	0,23
Cu	0,11	0,07	0,05
Nb	/	0,06	0,05
N	/	0,03	0,06
W	/		1,0

Conventional heat treatment of these steels consists of austenitizing and oil quenching, followed by one or two-step tempering. The microstructure obtained after the heat treatment is tempered martensite.

In addition, a non-conventional heat treatment was performed with the aim to obtain microstructure with different morphology of precipitates. The austenitizing

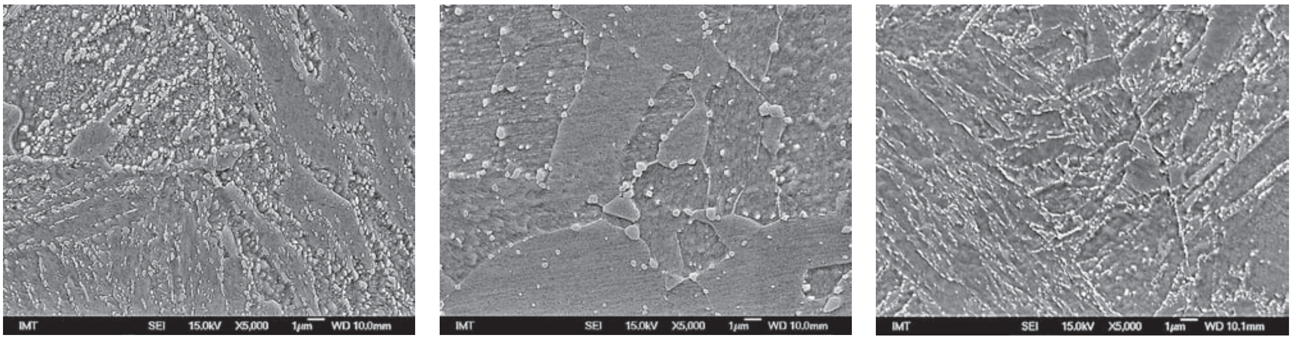

Figure 1 a) secondary electron image of microstructure of X20CrMoV12-1 steel after 2h of tempering,
b) microstructure of X10CrMoVNb9-1 steel after 400 h of tempering,
c) microstructure of X12CrMoWVNbN10-1-1 steel

of both X20CrMoV12-1 and X10CrMoVNb9-1 steels was performed at 1 050 °C followed by oil quenching. The next step was tempering for 2 hours at 740 °C and cooling in oil. The last step was tempering of both steels at 800 °C for 2 and 400 hours separately. The 2 h tempering was used to obtain a distribution of carbides in stringers along the grain boundaries and sub-grain boundaries, whereas the 400 h tempering was used to obtain a uniform distribution of particles.

In the case of the X12CrMoWVNbN10-1-1 steel, the austenitizing temperature was modified, by applying a higher and lower than the prescribed austenitizing temperature. Similarly, a higher and lower temperature than the prescribed tempering temperature were used. Details on austenitizing and tempering temperatures cannot be disclosed due to business confidentiality.

Creep tests were performed with constant load creep testing machines according to the standard SIST EN ISO 204, using testing temperatures between 550 °C and 650 °C and creep stress range of 170 to 230 MPa. All specimens were prepared in the longitudinal direction and taken at the ¼ of the diameter of material.

RESULTS AND DISCUSION

Microstructure

In order to analyze the carbide particles distribution, the microstructure of investigates steels was examined at magnifications of 5 k and 10 k. An example of the effect of different tempering times on the distribution and size of the precipitates is shown in Figure 1. After 2 h of tempering at 800 °C, the majority of precipitates can be noticed in stringers along the grain and subgrain boundaries (Figure 1a), while after 400 h of tempering, the distribution of precipitates is more uniform (Figure 1b). In the case of the steel X12CrMoWVNbN10-1-1 (Figure 1c) the differences due to variation in austenitizing and tempering temperatures cannot be seen as clearly as in the previous steels. The microstructure is tempered martensite with precipitates distributed mainly on grain boundaries and subgrain boundaries of martensitic laths.

A more detailed investigation of microstructure was carried out by automatic image analyses using Image J software [14]. 10 images were acquired at randomly chosen locations for each steel sample. This way, the number of precipitates, their average size, as well as their mutual spacing was determined.

With longer tempering times, the average number of carbide particles decreased from ~600 to ~400 particles per 100 µm^2 in the X20CrMoV12-1 steel (Figure 2). While in the X10CrMoVNb9-1 steel, it decreased from ~390 to 165 particles per 100 µm^2.

For the X12CrMoWVNbN10-1-1 steel the average number of precipitates increases from approximately 100 particles per 100 µm^2 for the lower austenitizing temperature to approximately 150 particles per 100 µm^2 for the higher temperature (Figure 3). Vice versa the average spacing between precipitates decreases with increasing austenitizing temperature from approximately 17 µm to 14 µm. As shown in Figure 3, tempering temperature has the opposite effect.

Creep rate

Creep tests were performed on the X20CrMoV12-1 and X10CrMoVNb9-1 steels after both tempering times with the aim to determine how different tempering durations influence the creep resistance. The secondary or steady-state creep rate was defined from the creep curve of each creep test. The dependence of steady-state creep rate on temperature for the investigated steels after 2 h and 400 h of tempering is shown in Figure 4a. The creep rate increases for both investigated steels with increasing

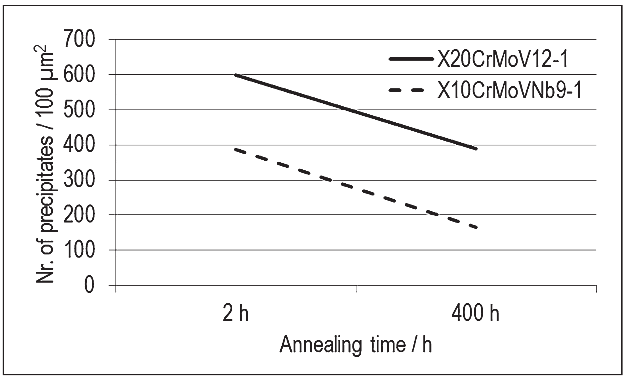

Figure 2 Decrease of number of precipitates with the longer time of tempering for the X20CrMoV12-1 and X10CrMoVNb9-1 steel

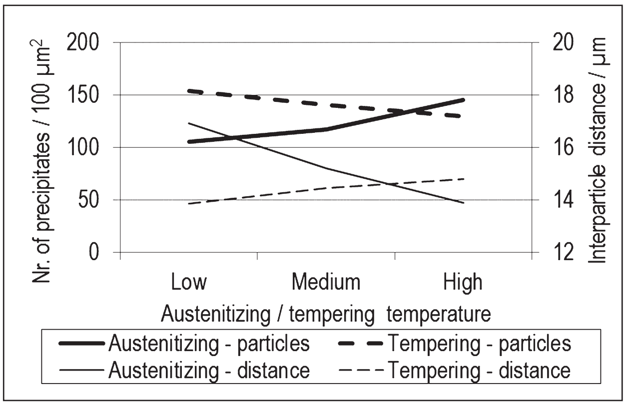

Figure 3 Dependence of the number of precipitates and interparticle spacing on austenitizing and second tempering temperature for the X12CrMoWVNbN10-1-1 steel

the creep test temperature at constant creep stress of 170 MPa, but the increase is more pronounced in the case of X10CrMoVNb9-1. The results of creep test performed at 650 °C for the X12CrMoWVNbN10-1-1 steel, show that the change of second tempering temperature (TT2) affects the creep resistance of the steel (Figure 4b).

The increase of tempering temperature leads to reduced number of precipitates, consequently the creep resistance is deteriorated. Results also confirm the fact that the creep rate increases not only with creep stress, but also with temperature of second tempering.

CONCLUSIONS

From the performed experiments and obtained results on the investigated steels, the following conclusions can be drawn:

- The number of precipitates decreases with longer tempering time for the X20CrMoV12-1 and X10CrMoVNb9-1 steels, consequently leading to increased steady state creep rate.
- For the X12CrMoWVNbN10-1-1 steel an increase of austenitizing temperature causes the increase of number of precipitates and at the same time the decrease in interparticle spacing.
- With the increase of temperature of second tempering, the creep rate increases.

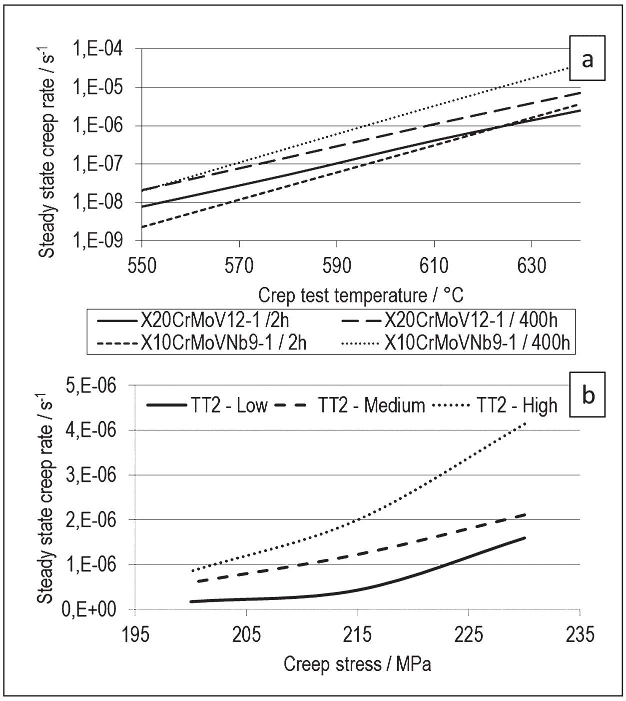

Figure 4 a) Dependence of steady-state creep rate on creep test temperature for the X20CrMoV12-1 and X10CrMoVNb9-1 steels for two different tempering durations, b) Dependence of steady-state creep rate on second tempering temperature (TT2) for the X12CrMoWVNbN10-1-1 steel

REFERENCES

[1] Mayer, K.-H.; Masuyama, F.; Creep resistant steels, Woodhead Publishing Limited and CRC Press LCC, USA, The development of creep-resistant steels, 2008, 15-70

[2] Abe, F.; Analysis of creep rates of tempered martensitic 9%Cr steel based on microstructure evolution, Materials Science and Engineering A 510 (2009), 64-69

[3] Kostka, A.; Tak, K.G.; Hellmig, R.J.; Estrin, Y.; Eggeler, G.; On the contribution of carbides and micrograin boundaries to the creep strength of tempered martensite ferritic steels, Acta Materialia 55 (2007) 2, 539-550

[4] Maruyama, K.; Sawada, K.; Koike, J.; Strengthening Mechanisms of Creep Resistant Tempered Martensitic Steel, ISIJ International 41 (2001) 6, 641-653

[5] Burja, J.; Tehovnik, F.; Medved, J.; Godec, M.; Knap, M.; Chromite Spinel Formation in Steelmaking Slags, Mater. Tehnol. 48 (2014) 5, 753-756

[6] Celin, R.; Burja, J.; Kosec, G.; A Comparison of As-Welded and Simulated Heat Affected Zone (HAZ) Microstructures, Mater. Tehnol. 50 (2016) 3, 455-460

[7] Skobir Balantič, D.A.; *Žužek,* B.; Vodopivec, F.; Grain boundaries of M23C6 particles in high chromium creep resistant steels, stability and effect on creep rate, Metalurgija 54 (2015) 3, 493-495

[8] Skobir, D.A.; Vodopivec, F.; Jenko, M.; Kosec, L.; Dražić, G.; An analysis of precipitates in X20CrMoV121 steel using the HR AES technique, Mater. Tehnol. 36 (2002) 6, 355-360

[9] Rapouch, J.; Bystriansky, J.; Sefl, V.; Svobodova, M.; Evaluation of The Structural Changes in 9 % Cr Creep-Resistant Steel Using an Electrochemical Technique, Mater. Tehnol. 49 (2015) 4, 543-548

[10] González, G.; Molina, R.; Delavalle, M.; Moro, L.; Variation of creep resistance in ferritic steels by a heat treatment, Procedia Materials Science 9 (2015), 412 - 418

[11] Vodopivec, F.; Skobir Balantič, D.A.; Jenko, M.; Žužek, B.; Godec, M.; Nucleation and growth of M23C6 particles in high-chromium creep-resistant steel, Mater. Tehnol. 46 (2012) 6, 633-636

[12] Vodopivec, F.; Kafexhiu, F.; Žužek, B.; Change of M23C6 particles size and spacing by tempering a high-chromium creep resistant steel at 800-550 °C, Steel Res. Int. 86 (2015) 3, 278–283

[13] Tehovnik, F.; Steiner Petrovič, D.; Vode, F.; Burja, J.; Influence of molybdenum on the hot-tensile properties of austenitic stainless steels, Mater. Tehnol. 46 (2012) 6, 649-655

[14] Bolte, S.; Cordelières, F.P.; A guided tour into subcellular colocalization analysis in light microscopy, Journal of Microscopy 224 (2006) 3, 213-232

Note: The responsible translator for English language is Marija Majda Travnik Vode, Slovenia